



General Palaeontology, Systematics and Evolution (Palaeobotany)

## Coryphoid palms from the Oligocene of China and their biogeographical implications



### *Palmiers coryphoïdés de l'Oligocène de Chine et leurs implications biogéographiques*

Qiu-Jun Wang<sup>a,b</sup>, Fu-Jun Ma<sup>a</sup>, Jun-Ling Dong<sup>a</sup>, Yi Yang<sup>a</sup>, Pei-Hong Jin<sup>a</sup>, Bai-Nian Sun<sup>a,b,\*</sup>

<sup>a</sup> School of Earth Sciences and Key Laboratory of Mineral Resources in Western China (Gansu Province), Lanzhou University, Lanzhou 730000, China

<sup>b</sup> Key Laboratory of Economic Stratigraphy and Palaeogeography, Nanjing Institute of Geology and Palaeontology, CAS, Nanjing 210008, China

#### ARTICLE INFO

##### Article history:

Received 17 June 2014

Accepted after revision 13 March 2015

Handled by Dimichele

##### Keywords:

Coryphoid palm

Oligocene

China

Biogeography

##### Mots clés :

Palmier coryphoïdé

Oligocène

Chine

Biogéographie

#### ABSTRACT

Fossil palm leaves from the Oligocene deposits in Ningming County, Guangxi, China, have been reported for the first time. The palmate leaf shape along with a definite costa support the placement of the fossils in the Coryphoideae. Three new species are described: *Chuniophoenix slenderifolia* sp. nov., *Livistona roundifolia* sp. nov. and *Trachycarpus formosa* sp. nov. The palm fossils belong to three taxa and indicate that palms in southern China began to diversify no later than the Oligocene and that a diversified palm flora was already present at that time in Guangxi. This report provides new information about the biogeographical history of Chinese palms over geological time.

© 2015 Académie des sciences. Published by Elsevier Masson SAS. All rights reserved.

#### R É S U M É

Des feuilles de palmiers fossiles en provenance de dépôts oligocènes du Comté de Ningming, Guangxi, Chine ont été enregistrées pour la première fois. La forme de la feuille de palmier, de même qu'une nervure bien définie sont des arguments pour placer ces fossiles au sein des Coryphoideae. Trois nouvelles espèces sont décrites : *Chuniophoenix slenderifolia* sp. nov., *Livistona roundifolia* sp. nov., et *Trachycarpus formosa*. Les fossiles de palmiers appartiennent à trois taxons et indiquent que les palmiers du Sud de la Chine ont commencé à se diversifier dès l'Oligocène et qu'une flore diversifiée de palmiers était déjà présente à cette époque dans le Guangxi. Cet enregistrement apporte de nouvelles informations sur l'histoire biogéographique des palmiers de Chine au cours des temps géologiques.

© 2015 Académie des sciences. Publié par Elsevier Masson SAS. Tous droits réservés.

\* Corresponding author. School of Earth Sciences, Lanzhou University, 222 South Tianshui Road, Lanzhou 730000, China.  
E-mail address: [bnsun@lzu.edu.cn](mailto:bnsun@lzu.edu.cn) (B.-N. Sun).

## 1. Introduction

Palms (Arecaceae) are among the oldest monocotyledonous flowering plants (Janssen and Bremer, 2004), currently comprising 184 genera with 2500 described species (Baker and Couvreur, 2013a, b; Dransfield et al., 2008; EBFC, 1991). The monophyly of Arecaceae is supported by phylogenetic studies (Dransfield et al., 2005; Janssen and Bremer, 2004), and five subfamilies are recognized within the group: Arecoideae, Calamoideae, Ceroxyloideae, Coryphoideae and Nypoideae (Asmussen et al., 2006; Dransfield et al., 2005, 2008). Palms have a pantropical distribution, with some species extending into the subtropics (Dransfield et al., 2008; EBFC, 1991; Ling, 2002; Tomlinson, 1979). Palms are also one of the most characteristic and ecologically important components of tropical rain forests (Baker and Couvreur, 2013a; Tomlinson, 1979), and they have served as a model system in biogeographical, ecological studies (Baker and Couvreur, 2013a; Eiserhardt et al., 2011) and rainforest evolution (Couvreur et al., 2011). Understanding how the biodiversity of palms is shaped through time may provide a basis to track rainforest evolution (Couvreur et al., 2011).

The phylogeny and biogeography of palms have been the subject of numerous studies (Baker and Couvreur, 2013b; Couvreur et al., 2011; Eiserhardt et al., 2011; Kissling et al., 2012), and fossil evidence can provide new insights in this regard. The history of fossil palms is summarized by Dransfield et al. (2008), and the earliest occurrence can be dated to the Aptian (Harley, 2006; Pan et al., 2006; Zhou et al., 2013). Palms have an extensive fossil record and are represented by a great number of fossil species, with nearly all parts of the plant having been recorded (Dransfield et al., 2008; Harley, 2006). However, palm fossils with sufficient diagnostic details, which can assess their natural affinities within Arecaceae, are rarely reported (Daghlian, 1978, 1981; Harley, 2006; Zhou et al., 2013). So, the lack of Oligocene palms in the world has restricted our interpretation of their biogeography and diversity at that time. Although the fossil record of palms in Asia is extensive (Dutta et al., 2011; EBCPC, 1978; Wei, 1995; Zhou et al., 1990), palm fossils from China are rare. Only five confirmed reports of palm fossils from China are known (Endo, 1934; Guo, 1965; Tao, 1988; Zhou et al., 1990, 2013). Thus, it is not clear whether the prevalence of extant Chinese palms corresponds to a recent diversification event or if it occurred over a longer geological period.

Recently, three fossil palm morphotypes with well-preserved cuticles were discovered from the Oligocene deposits in Ningming County, Guangxi, China. Since cuticle structure of palm fossils is poorly known (Daghlian, 1978; Kvaček and Herman, 2004; Zhou et al., 2013), the cuticle studies in this paper will provide additional morphological knowledge of fossil palms. The importance of the fossils on palm biogeography in China is also discussed. In addition, the fossil palms provide a new insight into the plant diversity of the Guangxi flora during the Oligocene.

## 2. Material and methods

The fossil material was collected from the Ningming Formation at 22°09'15.77"N, 107°01'23.11"E (Fig. 1) in the northwestern region of Chengzhong Town, Ningming County, Guangxi, China. The Ningming Formation consists of shallow lacustrine deposits, gray, dark gray mudstone with light yellow shaly siltstone and fine-grained sandstone (Fig. 2; Ning et al., 1994). The age of the Ningming Formation is regarded as Oligocene based on palynostratigraphy (Kuang et al., 2004; Wang et al., 2003), plant macrofossils (Li et al., 2003), well-preserved fishes (Chen and Chang, 2011; Chen et al., 2004, 2005) and lithostratigraphy (Li et al., 1995; Ning et al., 1994).

The experimental treatments for the fossil cuticles were well described in previous studies (Ma et al., 2013; Wang et al., 2013). Here, we followed these methods with slight modifications. The fossil material was immersed in 10% HCl for one day and then with 50% HF overnight. Cleaned samples were macerated using Schulze's solution, followed by 5% KOH to obtain cuticles. After rinsing with distilled water multiple times, some cuticles were stained with 1% safranin solution for light microscope (LM). Unstained cuticles were mounted on stubs and sputter-coated with gold for scanning electron microscope (SEM).

Extant palms for morphological and cuticular comparisons were collected from trees growing at the South China Botanical Garden, Chinese Academy of Sciences (IBSC). These cuticles were prepared according to the method of Wang et al. (2014). The material was immersed in a 1:1 solution of glacial acetic acid (CH<sub>3</sub>COOH) and 30% hydrogen peroxide (H<sub>2</sub>O<sub>2</sub>) and then placed in a hot water-bath at 80 °C for 10 h. Once the cuticles have turned white and transparent, they can easily be separated. The same procedures for LM preparations were then followed as the method for the fossil cuticles.

All specimens, LM slides, and SEM stubs are deposited at the Institute of Palaeontology and Stratigraphy, Lanzhou University, Gansu Province, China. Morphological descriptions of palm leaves are based on the terminology of EBFC (1991) and Read and Hickey (1972). The terms used by Dilcher (1974) and Wang and Tao (1991) were used for anatomical characters. The abbreviation LDGSW refers to the Institute of Palaeontology and Stratigraphy, Lanzhou University; HNZWY refers to the extant material from IBSC.

## 3. Results

### 3.1. Taxonomic identification of the Ningming palms

Palm leaves fall basically into two types, pinnate and palmate. The pinnate leaves are feather-like with a long stout rachis bounded on each side by a number of pinnae or leaflets (Dransfield et al., 2008; Zhou et al., 2013). Although pinnate leaves are found in each palm subfamily, they differ from the present fossils in leaf pattern. The palmate leaves are fan-shaped with segments radiating from the base of leaf blade and are characteristic of the subfamily Coryphoideae (Dransfield et al., 2008). Almost all coryphoid palms have palmate leaves, with

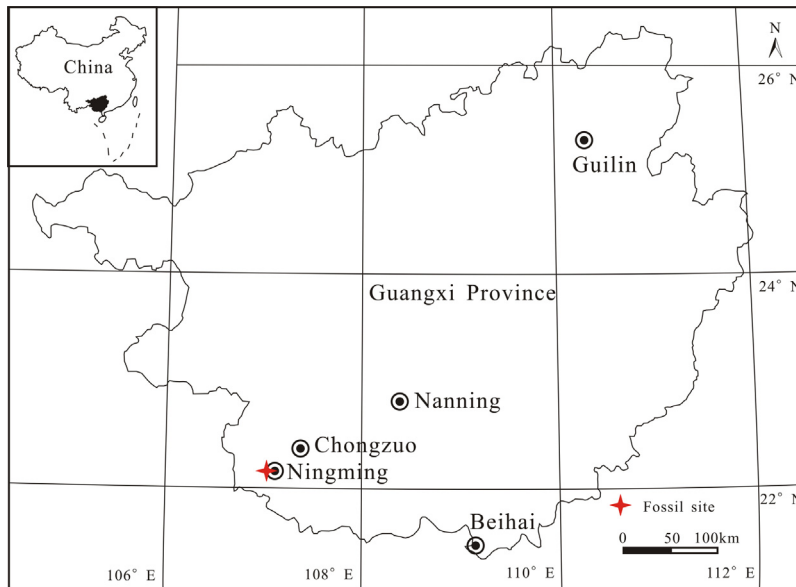


Fig. 1. Map showing the fossil locality (star).

Fig. 1. Carte montrant la localisation des fossiles (star).

the rare exception that members of the tribes Caryoteae and Phoeniceae possess pinnate leaves. Although palmate leaves are also present in some non-coryphoid palms, such as members of the tribes Lepidocaryeae and Mauritiinae (subfamily Calamoideae), these palms can be easily discounted for their leaf architectures (Dransfield et al., 2008; <http://www.palmweb.org/node/2>). Palmate leaves (Dransfield et al., 2008; Read and Hickey, 1972) are divided into the truly palmate type with no costa and the costapalmate type that has an extension of the petiole into the blade, forming a costa. In Coryphoideae, truly palmate leaves are rather unusual, while the costapalmate type is a more widespread (Dransfield et al., 2008; <http://www.palmweb.org/node/2>). Hence, the fossil palms from the Oligocene of Ningming are tentatively assigned to the subfamily Coryphoideae based on the palmate leaf shape with a definite costa.

The induplicate segment is also characteristic of coryphoid leaves (Dransfield et al., 2008), and is of crucial importance in systematics of fossil palms. However, leaf blades of the present palm fossils have only the basal portion preserved and the apex of segments are not preserved. It seems difficult to determine whether these leaves are induplicate or reduplicate. So, the insertion of the segments (induplication or reduplication) is not taken into account in the taxonomic identification of the Ningming palms.

Because of the great similarity in leaf morphology between palm genera (Read and Hickey, 1972), affinities between fossil palms and living genera are often difficult to determine. However, cuticles of palm leaves have been confirmed to possess much valuable information in generic assignment. For example, some palm leaves from the Eocene have been assigned directly to the extant genera *Sabal* and *Livistona* based on cuticular structure (Daghlian, 1978; Daghlian and Dilcher, 1972; Zhou et al.,

2013). Therefore, the cuticular characteristics of leaf blades and petioles have been taken into account to identify fossil palms in this paper. In addition, the presence and morphology of the armature on palm petioles can also be used to identify fossil palms, some of which can be assigned to extant genera (Daghlian, 1981; Menon, 1964; Pan et al., 2006; Read and Hickey, 1972). Based on the morphological and cuticular characteristics of leaf blades and petioles, we place these fossil palms in specific extant taxa instead of assigning them to fossil genera. A comparison of the main characteristics of the following fossils and related palm species is shown in Appendix A.

#### 4. Systematics

Order: ARECALES  
Family: ARECACEAE  
Subfamily: CORYPHOIDEAE

##### Fossil species

Three fossil species of Coryphoideae are described as follows. All the voucher specimens were collected from the same locality and stratigraphy, and they are deposited at LDGSW.

##### Type locality

Chengzhong Town, Ningming County, Guangxi, China (Fig. 1).

##### Stratigraphy and age

Ningming Formation, Oligocene

##### Repository

Institute of Palaeontology and Stratigraphy, Lanzhou University, Gansu Province, China.

Genus: *Chuniophoenix*

Species: *Chuniophoenix slenderifolia* Q.J. Wang et B.N.

##### Sun sp. nov.

(Fig. 3a–c; Fig. 4a–f; Fig. 9a, b)

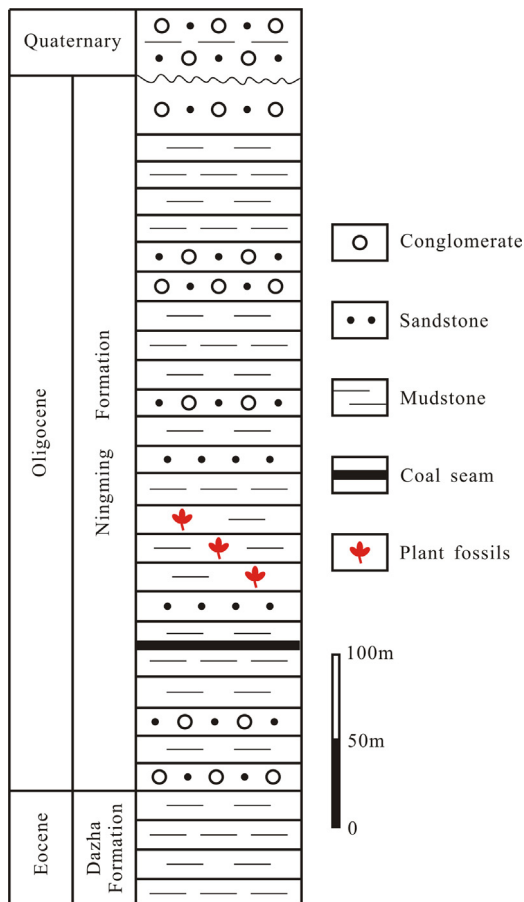


**Fig. 2.** Generalized stratigraphic section of the Ningming Formation (redrawn after Ning et al., 1994).

**Fig. 2.** Coupe stratigraphique généralisée de la formation Ningming (redessiné après Ning et al., 1994).

**Diagnosis:** Leaves costapalmate, fan-shaped; costa long and straight; petiole narrow, unarmed. Segments, sparse, emerging asymmetrically from the sides of the costa. Basal segments pendulous. Lamina isobilateral and amphistomatic; with stomatal complexes paratetracytic on the abaxial cuticle and brachyparatetracytic on the adaxial cuticle. Stomatal complexes cyclocytic on the petiole cuticle.

**Etymology:** The epithet *slenderifolia* is chosen for the leaf, which looks very slender in general morphology.

**Holotype:** LDGSW-2013-30-A, B (Fig. 3a and c) (designated here; part and counterpart specimens).

**Description:** The fossil is fan-shaped (Fig. 3a and c) with a portion of leaf blade and petiole preserved. The petiole exceeds 5.3 cm in length and 1.3 cm in width and is smooth and spineless, tapering upward to form a long straight costa (Fig. 3a and c; Fig. 9a). The costa is at least to 3.8 cm long (Fig. 3a and c). Segments, which emerge asymmetrically from the sides of the costa (Fig. 3a and c; Fig. 9a), are sparse and partially preserved. The basal segments are likely to be pendulous (Fig. 3a; Fig. 9a). Leaf blade divided into approximately 31 segments, which are no less than 7.9 cm long and 0.5–0.7 cm wide (Fig. 3a). Venation is parallel, with some faint, inconspicuous

ridges between the ribs of segments (Fig. 3b; Fig. 9b). The ridges may be probable lateral veins and are spaced 0.09–0.18 mm apart. Cross veins are not observed.

In the abaxial cuticle, ordinary epidermal cells (Fig. 4a and e) are regularly arranged in longitudinal files, narrowly rectangular to slender in outline, 5.65–21.54  $\mu\text{m}$  long and 5.08–12.00  $\mu\text{m}$  wide with a length/width (L/W) ratio from 0.5 to 5.6. Epidermal cells surrounding the stomata (Fig. 4d) are shorter and smaller. Stomatal complexes (Fig. 4d) are paratetracytic, 23.42–39.85  $\mu\text{m}$  long and 12.79–26.56  $\mu\text{m}$  wide, with 2 lateral and polar subsidiary cells. Guard cells (Fig. 4d) are irregularly rectangular, 16.07–18.00  $\mu\text{m}$  in length and 2.31–3.77  $\mu\text{m}$  in width, forming a slit-like aperture. Lateral subsidiary cells (Fig. 4d) are kidney-shaped, whereas polar subsidiary cells (Fig. 4d) are widely rectangular. Meanwhile, some stomatal complexes have 3 polar subsidiary cells with 2 at one end of the guard cells.

In the adaxial cuticle, epidermal cells (Fig. 4b) are arranged in longitudinal files more regularly, from rectangular or narrowly rectangular to irregularly polygonal in outline, mostly with rounded corners or perpendicular end walls, 6.45–30.00  $\mu\text{m}$  long and 2.35–23.55  $\mu\text{m}$  wide with a L/W ratio from 0.3 to 7.5. Anticlinal walls are straight, and periclinal walls may be smooth on the inner and outer surfaces (Fig. 4b). Stomatal complexes (Fig. 4b) are brachyparatetracytic, 22.61–33.23  $\mu\text{m}$  long and 10.43–27.42  $\mu\text{m}$  wide, with 2 lateral and polar subsidiary cells. Guard cells (Fig. 4b) are irregularly rectangular, 10.00–19.35  $\mu\text{m}$  in length and 1.74–4.52  $\mu\text{m}$  in width, forming a slit-like aperture. Lateral subsidiary cells (Fig. 4b) are kidney-shaped, whereas polar subsidiary cells (Fig. 4b) are wide rectangular. However, some stomatal complexes have irregular shapes, and their polar subsidiary cells are irregularly polygonal. Trichomes are not observed.

Epidermal cells of the petiole cuticle (Fig. 4c and f) are regularly arranged in longitudinal files, triangular, nearly square, rectangular or irregularly polygonal in outline, mostly with perpendicular end walls, 3.48–18.59  $\mu\text{m}$  long and 5.13–10.14  $\mu\text{m}$  wide with a L/W ratio from 0.4 to 2.6. Anticlinal walls of the epidermal cells are straight, and periclinal walls may be smooth on the inner and outer surfaces (Fig. 4c and f). Stomatal complexes (Fig. 4c and f) are typically cyclocytic, ranging from 20.51–35.90  $\mu\text{m}$  in diameter. They typically possess 6 lateral subsidiary cells, which are elongate (Fig. 4c and f). Trichomes are not observed.

Large damaged areas are commonly found on the leaf blade and petiole cuticles (Fig. 4c and e), consisting of many thin-walled cells. These cells are irregularly arranged, polygonal or isodiametric, 5.13–13.29  $\mu\text{m}$  long and 5.70–10.90  $\mu\text{m}$  wide, with a L/W ratio from 0.5 to 2.3. The damaged areas are similar to those observed on extant palms (Fig. 8h).

**Comparison:** Our material is assigned to the living genus *Chuniophoenix* based on the following similarities (Fig. 3a, c and d; Fig. 9a): asymmetrical leaf base, segments sparsely emerging from the sides of the costa, long straight costa with indistinct margins. Additionally, the cuticular characteristics of the leaf blade and petiole are also similar to those of extant *C. hainanensis* Burret, such as the paratetracytic stomatal complexes (Fig. 4a, d and g) and the shapes of epidermal cells (Fig. 4c, f and i). The most



**Fig. 3.** (Color online.) a–c: *Chuniophoenix slenderifolia* sp. nov.; d: *Chuniophoenix hainanensis*. a: foliage fragment, showing the basal portion of the leaf blade and the long straight costa with the indistinct margin (arrow); holotype, No. LDGSW-2013-30-A, scale bar = 1 cm; b: enlargement of a portion in “a”, showing the parallel venation and fine lateral veins (arrow); scale bar = 2 mm; c: basal portion of the counterpart of those in “a”; holotype, No. LDGSW-2013-30-B, scale bar = 1 cm; d: leaf of *Chuniophoenix hainanensis*, showing the indistinct margin (arrow); No. HNZWY-2013-QZ, scale bar = 1 cm.

**Fig. 3.** (Couleur en ligne.) a–c: *Chuniophoenix slenderifolia* sp. nov.; d: *Chuniophoenix hainanensis*. a: fragment de feuillage, montrant la portion basale d’une lame de feuille avec une nervure longue et droite à bords indistincts (flèche); holotype, n° LDGSW-2013-30-A, barre d’échelle = 1 cm; b: agrandissement d’une portion de « a », montrant un réseau de veines parallèles et de fines veines latérales (flèche); barre d’échelle = 2 mm; c: portion basale de la contre-empreinte de « a »; holotype, n° LDGSW-2013-30-B, barre d’échelle = 1 cm; d: feuille de *Chuniophoenix hainanensis*, montrant la marge indistincte (flèche); n° HNZWY-2013-QZ, barre d’échelle = 1 cm.

notable characteristic is the basal segments that emerge asymmetrically from the sides of the costa (Fig. 3a and c; Fig. 9a), which is very similar to that of *C. hainanensis* (Fig. 3d). However, *C. humilis* Burret, which is considered to

be costapalmate with a very small costa by some authorities (Henderson, 2009) or palmate by others (Dransfield et al., 2008), differs from the fossil in the distinctly narrow petiole (Fig. 10a) and cuticular characteristics (Fig. 10d

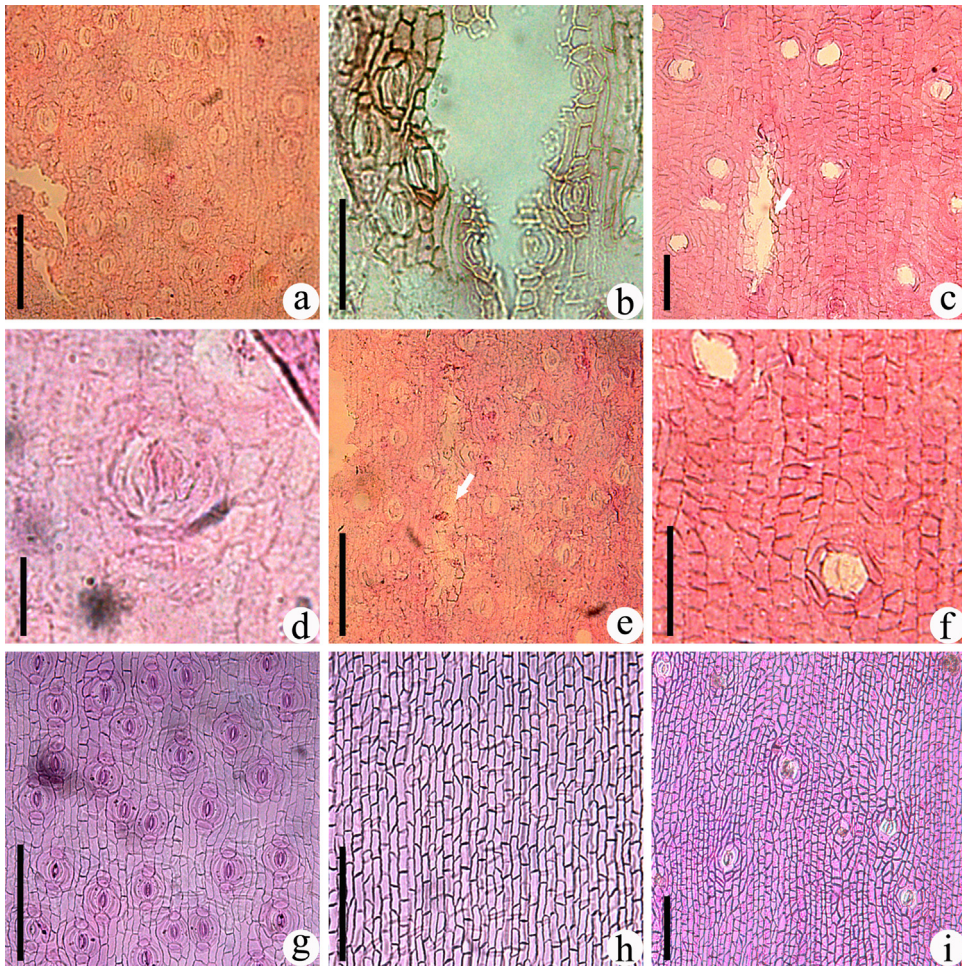


**Fig. 4.** (Color online.) a–f: *Chuniophoenix slenderifolia* sp. nov.; g–i: *Chuniophoenix hainanensis*. a: abaxial cuticle, showing paratrachytic stomata and epidermal cells; scale bar = 100  $\mu\text{m}$ ; b: adaxial cuticle, showing brachyparatrachytic stomata and epidermal cells; scale bar = 50  $\mu\text{m}$ ; c: petiole cuticle, showing cycloctytic stomata, epidermal cells, and the damaged area (arrow); scale bar = 50  $\mu\text{m}$ ; d: abaxial cuticle, showing the paratrachytic stoma; scale bar = 20  $\mu\text{m}$ ; e: abaxial cuticle, showing the damaged area (arrow); scale bar = 100  $\mu\text{m}$ ; f: petiole cuticle, showing the cycloctytic stoma; scale bar = 50  $\mu\text{m}$ ; g: abaxial cuticle, showing stomata and epidermal cells; scale bar = 100  $\mu\text{m}$ ; h: adaxial cuticle, showing epidermal cells; scale bar = 100  $\mu\text{m}$ ; i: petiole cuticle, showing stomata and epidermal cells; scale bar = 100  $\mu\text{m}$ .

**Fig. 4.** (Couleur en ligne.) a–f: *Chuniophoenix slenderifolia* sp. nov.; g–i: *Chuniophoenix hainanensis*. a: cuticule abaxiale, montrant des stomates paratrachytiques et des cellules épidermiques, barre d'échelle = 100  $\mu\text{m}$ ; b: cuticule adaxiale, montrant des stomates brachyparatrachytiques et des cellules épidermiques, barre d'échelle = 50  $\mu\text{m}$ ; c: cuticule de pétiole montrant des stomates cycloctytiques, des cellules épidermiques et la zone endommagée (flèche), barre d'échelle = 50  $\mu\text{m}$ ; d: cuticule abaxiale, montrant les stomates paratrachytiques; barre d'échelle = 20  $\mu\text{m}$ ; e: cuticule abaxiale, montrant la zone endommagée (flèche), barre d'échelle = 100  $\mu\text{m}$ ; f: cuticule de pétiole, montrant les stomates cycloctytiques, barre d'échelle = 50  $\mu\text{m}$ ; g: cuticule abaxiale, montrant des stomates et des cellules épidermiques, barre d'échelle = 100  $\mu\text{m}$ ; h: cuticule montrant des cellules épidermiques, barre d'échelle = 100  $\mu\text{m}$ ; i: cuticule de pétiole, montrant des stomates et des cellules épidermiques, barre d'échelle = 100  $\mu\text{m}$ .

and g). Asymmetrical leaf bases are also represented in other living Arecaceae (EBFC, 1991; Zhou et al., 2013), such as members of the genera *Bismarckia*, *Hyphaene*, *Latania* and *Sabal*. However, *Bismarckia*, which is a monotypic genus endemic to Madagascar, has a robust petiole (about 3.5–5.5 cm) and approximately 75 folded segments (Brown, 2013; <http://www.palmweb.org/node/2>). The petioles of extant *Hyphaene* are 2–6 cm wide and armed with robust, triangular spines (about 1–3.5 cm long and 1.5 cm wide) (<http://www.palmweb.org/node/2>). *Latania* is native to islands in the western Indian Ocean, whose leaves differ in possessing robust petioles ( $\geq 2$  cm) and broader segments (about 2.3–3.3 cm in width). Although

asymmetrical leaf bases are common in extant *Sabal*, such as *S. bermudana* L.H. Bailey, *S. mexicana* Mart. and *S. minor* (Jacq.) Pers. (Fig. 10c), these species differ in possessing a wide and robust petiole (about 2.2–3.3 cm) (the measurement data from the Herbarium Catalogue, Royal Botanic Garden, Kew). Moreover, their segments are much wider than that in the fossil and differ for their cuticular characteristics (Fig. 10e, f, h and i).

The asymmetrical leaf base is uncommon among fossil palm leaves. Only two *Sabalites* species, *S. asymmetricus* Jin et Zhou and *Sabalites* sp. from the Eocene of Hainan, China, are more or less similar to the new species in gross morphology. The former has more segments (26 pairs)

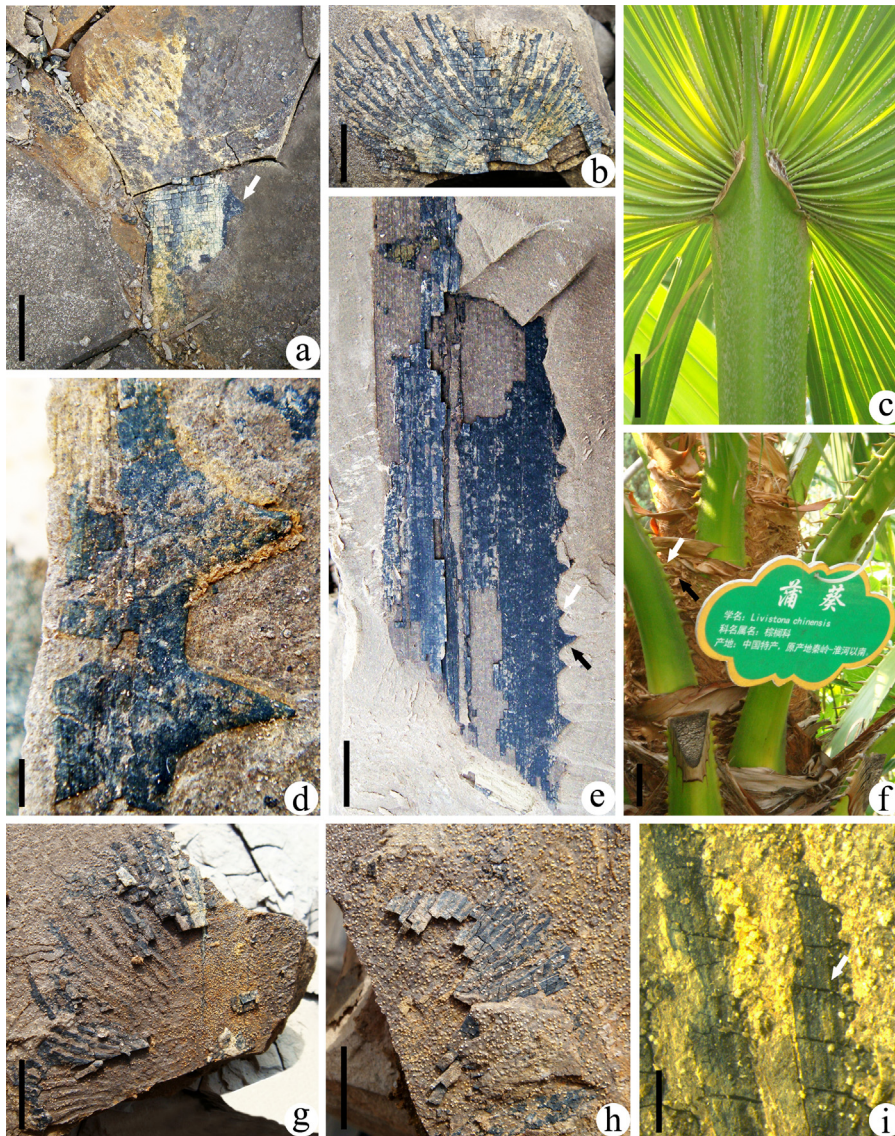


**Fig. 5.** (Color online.) a–b, d–e, g–i: *Livistona roundifolia* sp. nov.; c, f: *Livistona chinensis*. a: foliage fragment, showing the basal portion of the leaf blade and the robust spine (arrow); holotype, No. LDGSW-2013-66-A, scale bar = 2 cm; b: basal portion of the counterpart of those in “a”, showing the basal portion of the leaf blade with a distinct costa; holotype, No. LDGSW-2013-66-B, scale bar = 1 cm; c: leaf of *Livistona chinensis*; No. HNZWY-2013-PK, scale bar = 2 cm; d: a portion of petiole, showing two small spines; paratype, No. LDGSW-2013-89, scale bar = 2 mm; e: a larger portion of petiole, showing small (white arrow) and large spines (black arrow); paratype, No. LDGSW-2013-07, scale bar = 1 cm; f: the petiole of *Livistona chinensis*, showing small (white arrow) and large spines (black arrow); scale bar = 4 cm; g: foliage fragment with the costa; paratype, No. NM02-67, scale bar = 1 cm; h: foliage fragment; paratype, No. LDGSW-2013-68, scale bar = 1 cm; i: enlargement of a portion in “b”, showing the parallel venation (arrow); scale bar = 2 mm.

**Fig. 5.** (Couleur en ligne.) a–b, d–e, g–i: *Livistona roundifolia* sp. nov.; e, f: *Livistona chinensis*. a: fragment de feuillage montrant la portion basale d’une lame de feuille et une épine robuste (flèche); holotype, n° LDGSW-2013-66-A, barre d’échelle = 2 cm; b: portion basale de la contre-empreinte de « a », montrant la partie basale de la lame de feuille, avec une nervure distincte; holotype, n° LDGSW-66-B, barre d’échelle = 1 cm; c: feuille de *Livistona chinensis*; No. HNZWY-2013-PK, barre d’échelle = 2 cm; d: portion de pétiole, montrant deux petites épines; paratype, n° LDGSW-2013-89, barre d’échelle = 2 mm; e: portion plus grande de pétiole montrant de petites épines (flèche blanche) et de grandes épines (flèche noire); paratype, n° LDGSW-2013-07, barre d’échelle = 1 cm; f: pétiole de *Livistomna chinensis*, montrant de petites épines (flèche blanche) et de grandes épines (flèche noire), barre d’échelle = 4 cm; g: fragment de feuillage, avec la nervure; h: fragment de feuillage. Paratype n° LDGSW-2013-68, barre d’échelle = 1 cm; i: agrandissement d’une portion en « b », montrant les veines parallèles, barre d’échelle = 2 mm. Paratype, n° NM02-67 barre d’échelle = 1 cm.

and a wide petiole (Zhou et al., 2013). The basal segments of *Sabalites* sp. (Guo, 1965) are perpendicular to the petiole and differ from the pendulous basal segments of the new species (Fig. 5, a, d, e). Additionally, the costa of *Sabalites* sp. is more distinct (Guo, 1965) than that of our specimens. Despite some similar morphologies found on other

reported fossil and modern palms, there are some distinct differences observed between them and the new species (Appendix A). Therefore, the present palm fossil cannot be definitively assigned to a reported fossil or extant species and thus is described as a new species, *C. slenderifolia* sp. nov.

Genus: *Livistona*

Species: *Livistona roundifolia* Q.J. Wang et B.N. Sun sp. nov.

(Fig. 5a, b, d, e and g–i; Fig. 6a–g; Fig. 9c)

**Diagnosis:** Leaves costapalmate, fan-shaped; costa stout; petiole wide, armed with robust spines. The petiole spines varying in size and curved. Some of the spines forming extended, arcuate connections with adjacent spines. Segments, emerging symmetrically from the petiole apex and the bilateral sides of the costa. Basal segments emerge from the petiole apex at an obtuse angle, making the shape of the leaf base rounded. Lamina bifacial and hypostomatic; stomatal complexes brachyparacetracytic on the leaf cuticle and paratetracytic on the petiole cuticle.

**Etymology:** The epithet *roundifolia* is chosen for the basal segments, which emerge approximately from the petiole apex at an obtuse angle and make the shape of the leaf base rounded.

**Holotype:** LDGSW-2013-66-A, B (Fig. 5a and b) (designated here; part and counterpart specimens).

**Paratypes:** LDGSW-2013-07, LDGSW-2013-67, LDGSW-2013-68, LDGSW-2013-89 (Fig. 5h, d, g and e) (designated here)

**Description:** The holotype (Fig. 5a and b) preserves the basal portion of a fan-shaped leaf blade and the top of petiole. The petiole exceeds 11.6 cm in length (Fig. 5e) and 2.7 cm in width (Fig. 5a and e) and is smooth, tapering upward to form a stout costa (Fig. 5a and b; Fig. 9c). The petiole spines vary significantly in size (Fig. 5a, d and e) and are 3.19–5.69 mm in length, with large spines alternating with one or two small ones (Fig. 5e; Fig. 9c). The spines are spaced 2.84–3.29 mm apart along the petiole and are curved (Fig. 5d and e). The bases of the spines are 2.59–4.17 mm in width of the small ones, and 4.91–7.41 mm in width of the large ones. Some of the spines form extended, arcuate connections with adjacent spines (Fig. 5e). The costa (Fig. 5a and b; Fig. 9c) is at least to 3.2 cm long. Segments, which are partially preserved, emerge symmetrically from the petiole apex (Fig. 5a) and along the sides of the costa (Fig. 5a and b). The basal segments arise from the petiole apex at an obtuse angle, and the shape of the leaf base is nearly rounded (Fig. 5a and b; Fig. 9c). Segments, approximately 32 pairs (Fig. 5a and b), are no less than 4.5 cm long (Fig. 5a). Venation is parallel and lateral veins are faint, spaced 0.45–0.51 mm apart (Fig. 5i). Cross veins are not observed.

Leaves are hypostomatic. The stomatal complexes (Fig. 6a, d and g) are typically brachyparacetracytic, 24.71–33.53  $\mu\text{m}$  long and 18.24–27.33  $\mu\text{m}$  wide, with 2 lateral and polar subsidiary cells. Guard cells (Fig. 6a and d) are crescent-shaped, 14.71–17.06  $\mu\text{m}$  in length and 1.76–2.94  $\mu\text{m}$  in width, forming a slightly wide aperture (Fig. 6a, d and g). Lateral subsidiary cells (Fig. 6a and d) are irregularly rectangular, whereas polar subsidiary cells (Fig. 6a and d) are wide rectangular.

In the abaxial cuticle, ordinary epidermal cells (Fig. 6a and d) are more or less regularly arranged in longitudinal files, from sub-square or rectangular to irregularly polygonal in outline, mostly with oblique end walls, 6.83–16.50  $\mu\text{m}$  long and 5.29–13.00  $\mu\text{m}$  wide with a L/W ratio from 0.8 to 2.4. Epidermal cells of the adaxial cuticle

(Fig. 6b and e) are more regularly arranged in longitudinal files, sub-square, rectangular, triangular, isodiametric, or irregularly polygonal in outline, mostly with sharp corners or oblique end walls, 5.06–16.29  $\mu\text{m}$  long and 6.18–11.24  $\mu\text{m}$  wide with a L/W ratio from 0.5 to 1.8. Anticlinal walls are straight and strongly cutinized, forming prominent flanges on the inner surface (Fig. 6e), whereas periclinal walls are smooth on the inner and outer surfaces (Fig. 6b and e). Trichomes are not observed.

Cuticles of the petiole are thicker. Epidermal cells (Fig. 6c) are similar to those of the adaxial cuticle in morphology but are more rectangular to elongate or slightly elongate, arranged in regularly longitudinal files, 3.08–12.12  $\mu\text{m}$  long and 2.15–8.18  $\mu\text{m}$  wide with a L/W ratio from 0.9 to 2.7. Anticlinal walls (Fig. 6c) are straight, whereas periclinal walls may be smooth on the inner and outer surfaces. Stomatal complexes (Fig. 6c and f) are paratetracytic, 14.15–30.30  $\mu\text{m}$  long and 10.46–19.55  $\mu\text{m}$  wide, with 2 lateral and polar subsidiary cells. Guard cells (Fig. 6c and f) are elongate, 10.46–20.12  $\mu\text{m}$  in length and 1.82–3.05  $\mu\text{m}$  in width, forming a slightly wide aperture (Fig. 6f). Lateral subsidiary cells (Fig. 6c and f) are crescent-shaped, but polar subsidiary cells (Fig. 6c and f) are inconspicuous, with ill-marked ridges. Trichomes are not observed.

Similarly large damaged areas are also found on the petiole cuticle (Fig. 6c). These thin-walled cells are 3.69–5.23  $\mu\text{m}$  long and 3.07–3.08  $\mu\text{m}$  wide, with a L/W ratio from 1.2 to 1.7.

**Comparison:** The present fossil is attributed to the genus *Livistona* primarily based on the following characteristics of the spines (Fig. 5a, d and e; Fig. 9c):

- they vary significantly in size with large ones alternating with small ones;
- they are robust, curved and generally uniform in size, shape and spacing;
- some of them form extended, arcuate connections with adjacent spines.

All these characteristics are well corresponded to the petiole spines of extant *L. chinensis* (Jacq.) R.Br. ex Mart. (Fig. 5f). In addition, the fossil shows some similarities to extant *Livistona* in the anatomical characters of the leaf blade and petiole. Firstly, the anticlinal walls of the epidermal cells are strongly cutinized for the fossil and extant *L. saribus* (Lour.) Merr. ex A.Chev. (Fig. 6k). Second, the stomatal complexes of the petioles all are paratetracytic between the present material and *L. saribus* (Fig. 6f and l). According to Read and Rickey (1972), the petioles of *Sabalites* and *Palmacites* are unarmed, and thus, the taxon does not belong to these fossil genera. Although armed petioles are common in extant *Borassus*, *Hyphaene*, *Satranala*, *Trachycarpus* and *Licuala*, there are some evident differences between them and the present fossil. The petiole teeth of *Borassus* can be divided into two types: large (0.3–2.8 cm long) and small serrate (0.1–0.85 cm long). The two types of teeth usually are heavily armed on the petiole margins (Dransfield et al., 2008; <http://www.palmweb.org/node/2>). The petiole spines of extant *Hyphaene*, which are generally uniform



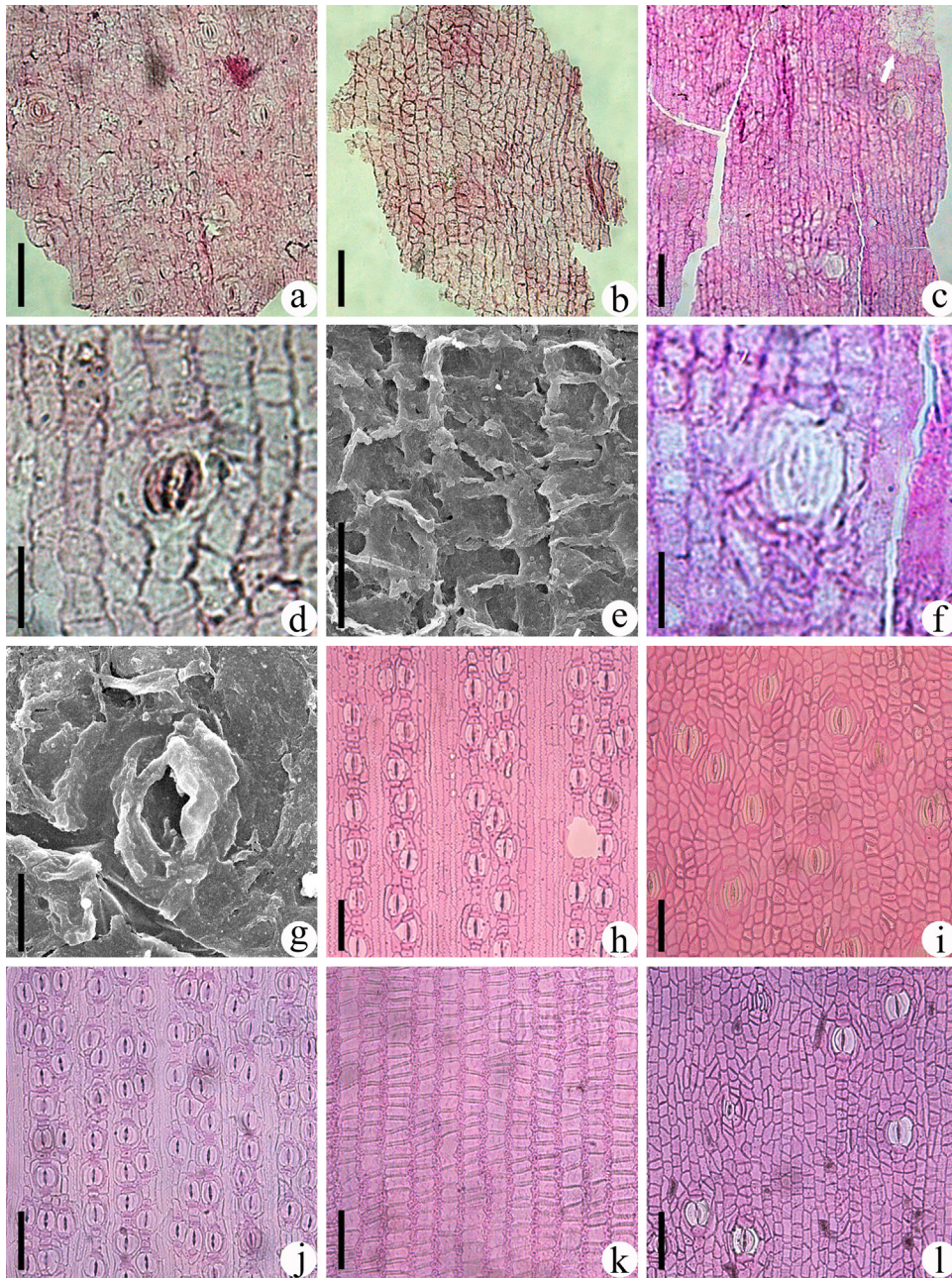


**Fig. 6.** a–g: *Livistona roundifolia* sp. nov.; h–i: *Livistona chinensis*; j–l: *Livistona saribus*. a: abaxial cuticle, showing brachyparatetracytic stomata and epidermal cells; scale bar = 50  $\mu\text{m}$ ; b: adaxial cuticle, showing epidermal cells; scale bar = 50  $\mu\text{m}$ ; c: petiole cuticle, showing paratetracytic stomata, epidermal cells, and the damaged area (arrow); scale bar = 20  $\mu\text{m}$ ; d: abaxial cuticle, showing the brachyparatetracytic stoma; scale bar = 20  $\mu\text{m}$ ; e: inner surface view of the adaxial cuticle, showing the epidermal cells with strongly cutinized anticlinal walls and smooth periclinal walls; scale bar = 20  $\mu\text{m}$ ; f: petiole cuticle, showing the paratetracytic stoma; scale bar = 20  $\mu\text{m}$ ; g: a stoma of the abaxial cuticle in outer side view; scale bar = 10  $\mu\text{m}$ ; h: abaxial cuticle, showing stomata and epidermal cells; scale bar = 50  $\mu\text{m}$ ; i: petiole cuticle, showing stomata and epidermal cells; scale bar = 50  $\mu\text{m}$ ; j: abaxial cuticle, showing stomata and epidermal cells; scale bar = 50  $\mu\text{m}$ ; k: adaxial cuticle, showing epidermal cells; scale bar = 50  $\mu\text{m}$ ; l: petiole cuticle, showing stomata and epidermal cells; scale bar = 50  $\mu\text{m}$ .

**Fig. 6.** a–g: *Livistona roundifolia* sp. nov.; h–i: *Livistona chinensis*; j–l: *Livistona saribus*. a: cuticule abaxiale, montrant des stomates brachytétracytiques et des cellules épidermiques; barre d'échelle = 50  $\mu\text{m}$ ; b: cuticule adaxiale, montrant des cellules épidermiques; barre d'échelle = 50  $\mu\text{m}$ ; c: cuticule de pétiole, montrant des stomates paratétracytiques, des cellules épidermiques et la zone endommagée (flèche), barre d'échelle = 20  $\mu\text{m}$ ; d: cuticule abaxiale, montrant les stomates brachyparatétracytiques, barre d'échelle = 20  $\mu\text{m}$ ; e: vue de la face interne de la cuticule adaxiale, montrant les cellules épidermiques avec des parois bombées intensément cutinisées et des parois enfoncées lisses, barre d'échelle = 20  $\mu\text{m}$ ; f: cuticule de pétiole montrant le stome paratétracytique, barre d'échelle = 20  $\mu\text{m}$ ; g: stomate de la cuticule abaxiale, vu du côté externe, barre d'échelle = 10  $\mu\text{m}$ ; h: cuticule abaxiale, montrant les stomates et les cellules épidermiques, barre d'échelle = 50  $\mu\text{m}$ ; i: cuticule de pétiole, montrant les stomates et les cellules épidermiques, barre d'échelle = 50  $\mu\text{m}$ .

in size (1–3.5 cm long and 1.5 cm wide) and shape (triangular), distinctly differ from the spines of the present species. *Satranala*, which is endemic to Madagascar, has armed petioles with minutely irregular teeth (Dransfield et al., 2008; <http://www.palmweb.org/node/2>). Extant *Trachycarpus* species are armed with very fine teeth on the petioles (EBFC, 1991; Dransfield et al., 2008; <http://www.palmweb.org/node/2>). The teeth of *Satranala* and *Trachycarpus* are not curved and noticeably acute, but minutely rounded or verrucate. The petioles of *Licuala* are no more than 1.5 cm in width (personal observation), which are narrower than those of our fossil.

The presence of spines on the petiole margins is uncommon among palm fossils. A few *Hyphaene* fossils with spiny petioles preserved are reported from the Oligocene of Ethiopia (Pan et al., 2006): *H. kappelmannii* A.D. Pan, B.F. Jacobs, J. Dransf. & W.J. Baker and *Hyphaene* sp. However, *H. kappelmannii* is characterized by the presence of noticeably curved spines on the narrow petiole. Petioles referred to *Hyphaene* sp. differ in possessing sharp spines. *L. tibetica* Tao from the Eocene of Xizang (Tao, 1988; Appendix B) and *Livistona* sp. from the Eocene of Hainan (Zhou et al., 2013), which lack detailed cuticular and morphological analysis, respectively, cannot be readily compared with the fossil.

Based on comparisons with other fossils and modern palms (Appendix A), a new specific name is proposed for the present fossil palm, *L. roundifolia* sp. nov.

#### Genus: *Trachycarpus*

Species: *Trachycarpus formosa* Q.J. Wang et B.N. Sun sp. nov.

(Fig. 7a–e; Fig. 8a–g; Fig. 9d, e)

**Diagnosis:** Leaves costapalmate, fan-shaped; costa robust, triangular; petiole wide. Segments, emerging symmetrically from the petiole apex and the bilateral sides of the costa. Leaf base cordate. Lamina bifacial and hypostomatic; stomatal complexes paratetracytic on the leaf cuticle and brachyparacytic on the petiole cuticle.

**Etymology:** The epithet *formosa* is chosen for the basal segments, which make the leaf blade beautiful and finely formed.

**Holotype:** LDGSW-2013-03-A, B (Fig. 7a and b) (designated here; part and counterpart specimens).

**Paratypes:** LDGSW-2013-77-A, B (Fig. 7c and d) (designated here; part and counterpart specimens).

**Description:** The fossil is fan-shaped (Fig. 7a and b) with the basal portion of leaf blade and the top of petiole preserved. The petiole (Fig. 7a) exceeds 5.1 cm long and 3.1 cm wide, smooth, tapering upward to form a robust costa (Fig. 7a and b; Fig. 9d). The costa is nearly triangular and 3.5 cm long (Fig. 7a and b). Segments, which are partially preserved, emerge symmetrically from the petiole apex (Fig. 7a and b) and along the sides of the costa (Fig. 7a–d). The basal segments (Fig. 7a and b; Fig. 9d) first curve obviously downward and then strongly upward, and the leaf base is cordate. Segments, approximately 40 pairs (Fig. 7a), are no less than 8.6 cm long and 1.3 cm wide. Venation is parallel (Fig. 7e), with lateral veins faint (Fig. 7e; Fig. 9e) and spaced 0.65–1.02 mm apart. Cross veins (Fig. 7e; Fig. 9e) connect two adjacent parallel

veins and most are oblique to them, spaced 1.16–2.96 mm apart.

The leaves are hypostomatic, and stomatal complexes (Fig. 8a, d and g) are paratetracytic, 30.86–43.68  $\mu\text{m}$  long and 19.19–32.50  $\mu\text{m}$  wide, with 2 lateral and polar subsidiary cells. Guard cells (Fig. 8d and g) are elongate, 18.55–22.22  $\mu\text{m}$  in length and 3.87–8.02  $\mu\text{m}$  in width, forming a slit-like aperture. Lateral subsidiary cells (Fig. 8d) are reniform, whereas polar subsidiary cells are wide rectangular.

Ordinary epidermal cells of the abaxial cuticle (Fig. 8a) are more or less regularly arranged in longitudinal files, rectangular to irregularly polygonal in outline, mostly with perpendicular end walls, 7.41–20.37  $\mu\text{m}$  long and 4.32–11.11  $\mu\text{m}$  wide with a L/W ratio from 0.7 to 4.1. The epidermal cells surrounding the stomata (Fig. 8d and g) are shorter and smaller than ordinary ones. Epidermal cells of the adaxial cuticle (Fig. 8b and e) are similar to those of the abaxial cuticle in morphology but are more regularly arranged in longitudinal files (Fig. 8h), 7.54–24.05  $\mu\text{m}$  long and 5.06–10.13  $\mu\text{m}$  wide with a L/W ratio from 0.9 to 3.5. Anticlinal walls of the epidermal cells on both cuticles are straight, with some strongly cutinized, and they form prominent flanges on the inner surface (Fig. 8e and g). Periclinal walls are smooth on the inner and outer surfaces (Fig. 8a, b, d, e, g). No trichomes are observed.

In the petiole cuticle, epidermal cells (Fig. 8c) are more regularly arranged in longitudinal files, rectangular, irregularly polygonal in outline, mostly with rounded corners or oblique end walls, 9.76–32.93  $\mu\text{m}$  long and 4.88–8.13  $\mu\text{m}$  wide with a L/W ratio from 1.3 to 4.5. Anticlinal walls are straight, whereas periclinal walls may be smooth on the inner and outer surfaces (Fig. 8c). Stomatal complexes (Fig. 8c and f) are brachyparacytic, 30.00–48.13  $\mu\text{m}$  long and 23.13–36.25  $\mu\text{m}$  wide. They bear only 2 lateral subsidiary cells, with polar subsidiary cells absent or inconspicuous (Fig. 8f). Guard cells (Fig. 8c and f) are elongate, 18.13–21.95  $\mu\text{m}$  in length and 1.88–4.27  $\mu\text{m}$  in width, forming a slit-like aperture. Subsidiary cells (Fig. 8f) are fusiform. Trichomes were not observed.

Large damaged areas are also found on the leaf blade and petiole cuticles (Fig. 8b and c). These thin-walled cells are 7.14–19.48  $\mu\text{m}$  long and 4.38–11.69  $\mu\text{m}$  wide, with a L/W ratio from 1.0 to 3.1.

**Comparison:** The present fossil is placed in the living genus *Trachycarpus* primarily based on the triangular costa and the anatomical characters. Moreover, the fossil and *T. fortunei* have similar venation patterns (Fig. 7e and g; Fig. 9e). The triangular costa can be appropriately compared with that of *T. fortunei* (Hooker) H. Wendland (Fig. 7a and f). Although similarly triangular costa can be also found between other fossil and extant palms, there are differences between these palms and the present material. *S. campbelli* (Newberry) Lesquereux, from the Paleo-Eocene of America (Lesquereux, 1878; Newberry, 1898), differs from the present material in possessing truncate leaf base (Guo, 1965; EBCPC, 1978). *S. zsei* Guo, from the Eocene of China (Guo, 1965; Zhou et al., 2013), is different in the following aspects: the segments are no more than 5 mm in width; and the petiole are ridged. Besides, the cordate leaf base (Fig. 7a and b) rarely occurs in the fossil

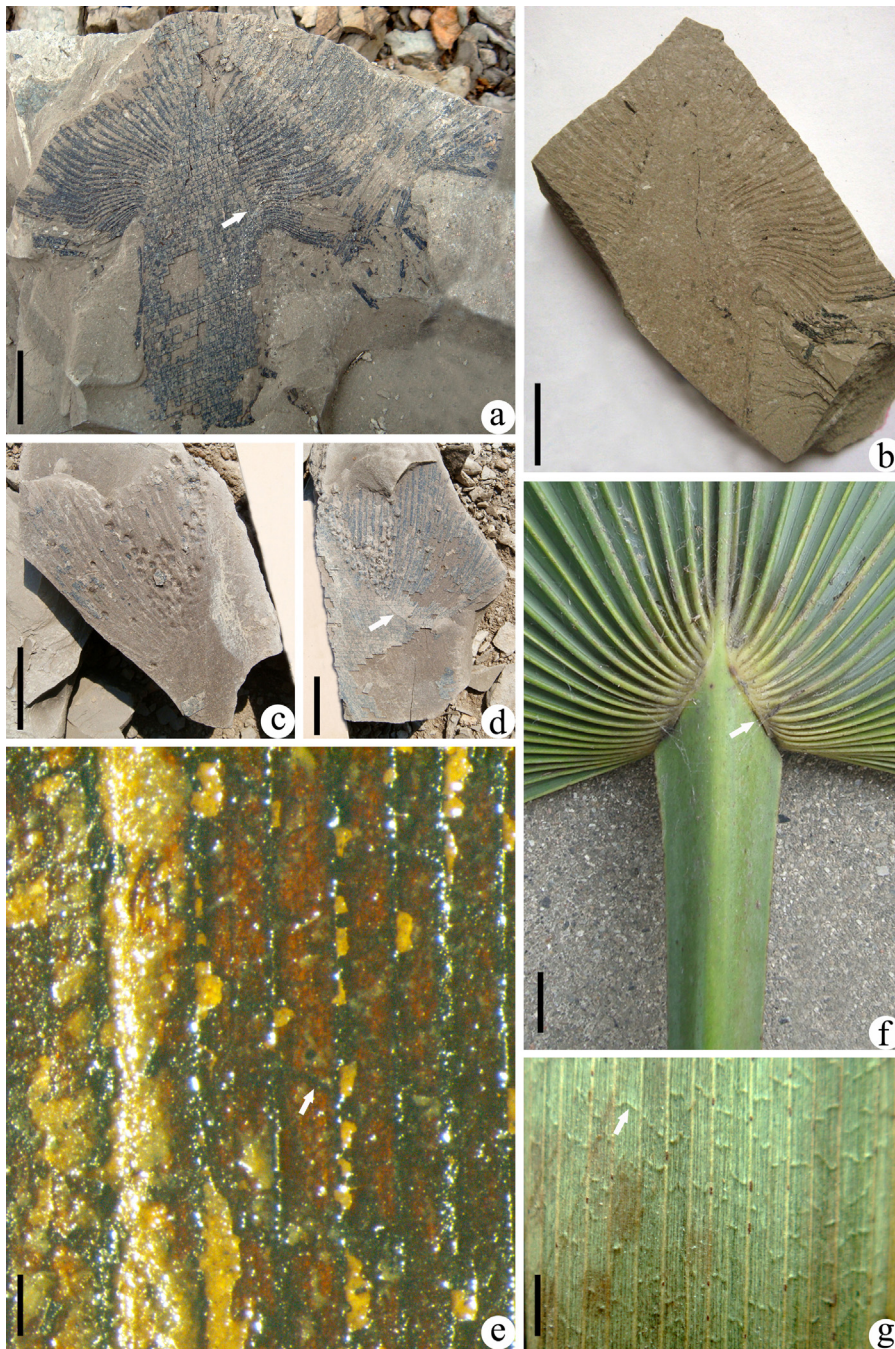


**Fig. 7.** (Color online.) a–e: *Trachycarpus formosa* sp. nov.; f–g: *Trachycarpus fortunei*. a: foliage fragment, showing the basal portion of the leaf blade and the triangular costa with the indistinct margin (arrow); holotype, No. LDGSW-2013-03-A, scale bar = 2 cm; b: basal portion of the counterpart of those in “a”, showing the general leaf morphology; holotype, No. LDGSW-2013-03-B, scale bar = 2 cm; c: foliage fragment with the costa; paratype, No. LDGSW-2013-77-A, scale bar = 2 cm; d: foliage fragment, showing the costa with the indistinct margin (arrow); paratype, No. LDGSW-2013-77-B, scale bar = 2 cm; e: enlargement of a portion in “a”, showing the parallel venation and cross veins (arrow); scale bar = 1 mm; f: leaf of *Trachycarpus fortunei*, showing the triangular costa with the indistinct margin (arrow); No. HNZWY-2013-ZL, scale bar = 2 cm; g: enlargement of a portion in “f”, showing parallel venation and cross veins (arrow); scale bar = 2 mm.

**Fig. 7.** (Couleur en ligne.) a–c: *Trachycarpus formosa* sp. nov.; f–g: *Trachycarpus fortunei*. a: fragment de feuillage montrant la portion basale de la lame de feuille et la nervure triangulaire avec sa marge indistincte (flèche); holotype, n° LDGSW-03-A, barre d'échelle = 2 cm; b: portion basale de la contre-empainte en « a », montrant la morphologie générale de la feuille; holotype, n° LDGSW-2013-03-B, barre d'échelle = 2 cm; c: fragment de feuillage avec la nervure; paratype, n° LDGSW-2013-77-A, barre d'échelle = 2 cm; d: fragment de feuillage, montrant la nervure avec sa marge indistincte (flèche); paratype, n° LDGSW-2013-77-B, barre d'échelle = 2 cm; e: agrandissement de la portion de « a », montrant le réseau parallèle de veines et des veines croisées (flèche); barre d'échelle = 1 mm; f: feuille de *Trachycarpus fortunei* montrant la nervure triangulaire avec sa marge indistincte (flèche); n° HNZWY-2013-ZL, barre d'échelle = 2 cm; g: agrandissement d'une portion de « f », montrant le réseau de veines parallèles et les veines croisées (flèche), barre d'échelle = 2 mm.

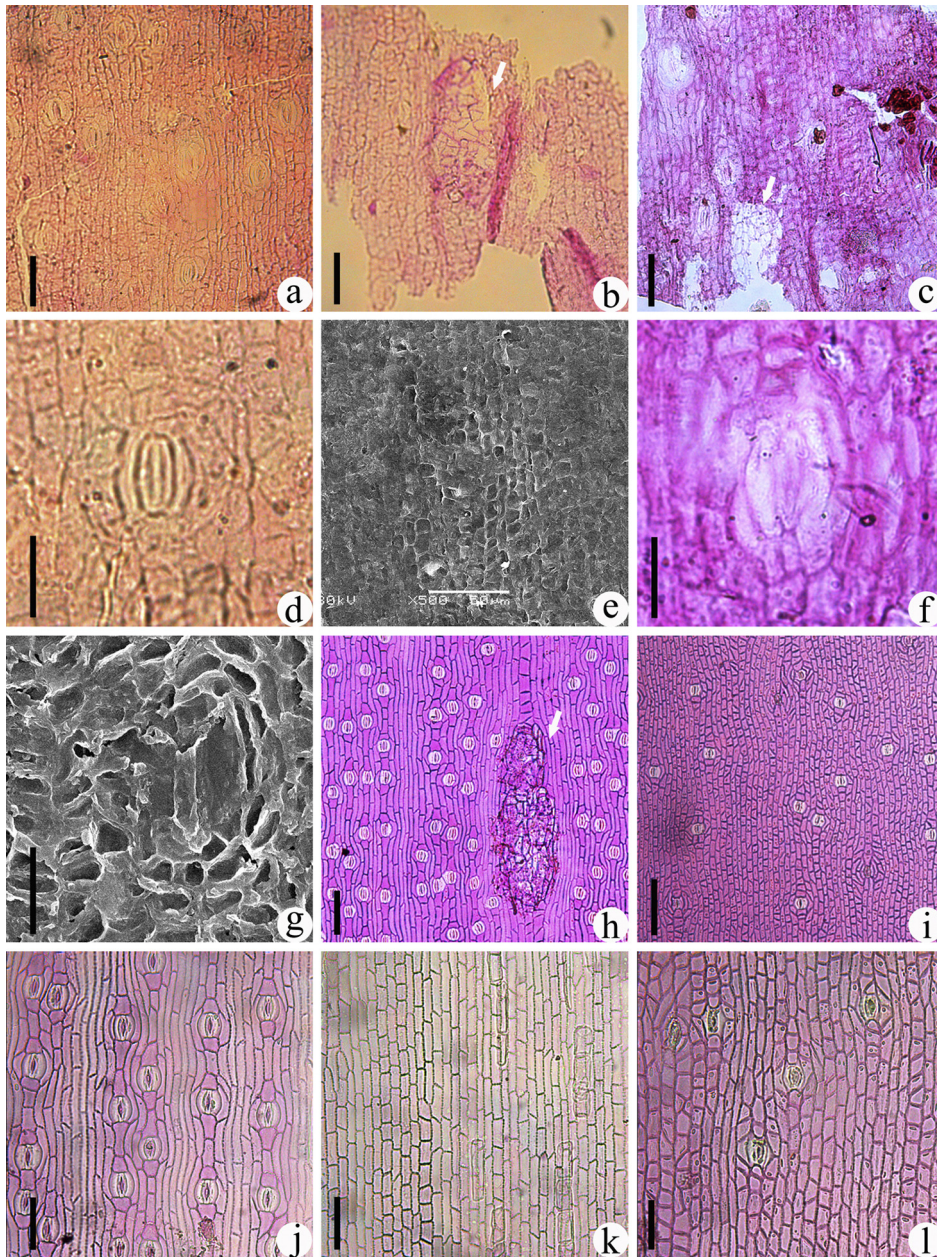


**Fig. 8.** (Color online.) a–g: *Trachycarpus formosa* sp. nov.; h–i: *Trachycarpus fortunei*; j–l: *Trachycarpus martianus*. a: abaxial cuticle, showing paratrachytic stomata and epidermal cells; scale bar = 50  $\mu\text{m}$ ; b: adaxial cuticle, showing epidermal cells and the damaged area (arrow); scale bar = 50  $\mu\text{m}$ ; c: petiole cuticle, showing brachyparacytic stomata, epidermal cells, and the damaged area (arrow); scale bar = 50  $\mu\text{m}$ ; d: abaxial cuticle, showing the paratrachytic stoma; scale bar = 20  $\mu\text{m}$ ; e: inner surface view of the adaxial cuticle, showing the epidermal cells with strongly cutinized anticlinal walls and smooth periclinal walls; scale bar = 50  $\mu\text{m}$ ; f: petiole cuticle, showing brachyparacytic stoma; scale bar = 20  $\mu\text{m}$ ; g: a stoma of the abaxial cuticle in inner side view; scale bar = 20  $\mu\text{m}$ ; h: abaxial cuticle, showing stomata, epidermal cells and the damaged area (arrow); scale bar = 50  $\mu\text{m}$ ; i: petiole cuticle, showing stomata and epidermal cells; scale bar = 50  $\mu\text{m}$ ; j: abaxial cuticle, showing stomata and epidermal cells; scale bar = 50  $\mu\text{m}$ ; k: adaxial cuticle, showing epidermal cells; scale bar = 50  $\mu\text{m}$ ; l: petiole cuticle, showing stomata and epidermal cells; scale bar = 50  $\mu\text{m}$ .

**Fig. 8.** (Couleur en ligne.) a–g: *Trachycarpus formosa* sp. nov.; h–i: *Trachycarpus fortunei*; j–l: *Trachycarpus martianus*. a : cuticule abaxiale, montrant des stomates paratrachytiques et des cellules épidermiques, barre d'échelle = 50  $\mu\text{m}$ ; b : cuticule adaxiale, montrant des cellules épidermiques et la zone endommagée (flèche), barre d'échelle = 50  $\mu\text{m}$ ; c : cuticule de pétiole, montrant des stomates brachyparacytiques, des cellules épidermiques et la zone endommagée (flèche); barre d'échelle = 50  $\mu\text{m}$ ; d : cuticule abaxiale, montrant les stomates paratrachytiques, barre d'échelle = 20  $\mu\text{m}$ ; e : vue de la surface interne de la cuticule adaxiale, montrant les cellules épidermiques avec les parois bombées intensément cutinisées, et les parois enfoncées lisses, barre d'échelle = 50  $\mu\text{m}$ ; f : cuticule de pétiole, montrant des stomates brachyparacytiques, barre d'échelle = 20  $\mu\text{m}$ ; g : un stomate de la cuticule abaxiale vu sur la face interne, barre d'échelle = 20  $\mu\text{m}$ ; h : cuticule abaxiale, montrant des stomates, des cellules épidermiques et la zone endommagée (flèche); barre d'échelle = 50  $\mu\text{m}$ ; i : cuticule de pétiole, montrant des stomates et des cellules épidermiques, barre d'échelle = 50  $\mu\text{m}$ ; j : cuticule abaxiale, montrant des stomates et des cellules épidermiques; barre d'échelle = 50  $\mu\text{m}$ ; k : cuticule adaxiale, montrant des cellules épidermiques, barre d'échelle = 50  $\mu\text{m}$ ; l : cuticule de pétiole, montrant ces stomates et des cellules épidermiques, barre d'échelle = 50  $\mu\text{m}$ .

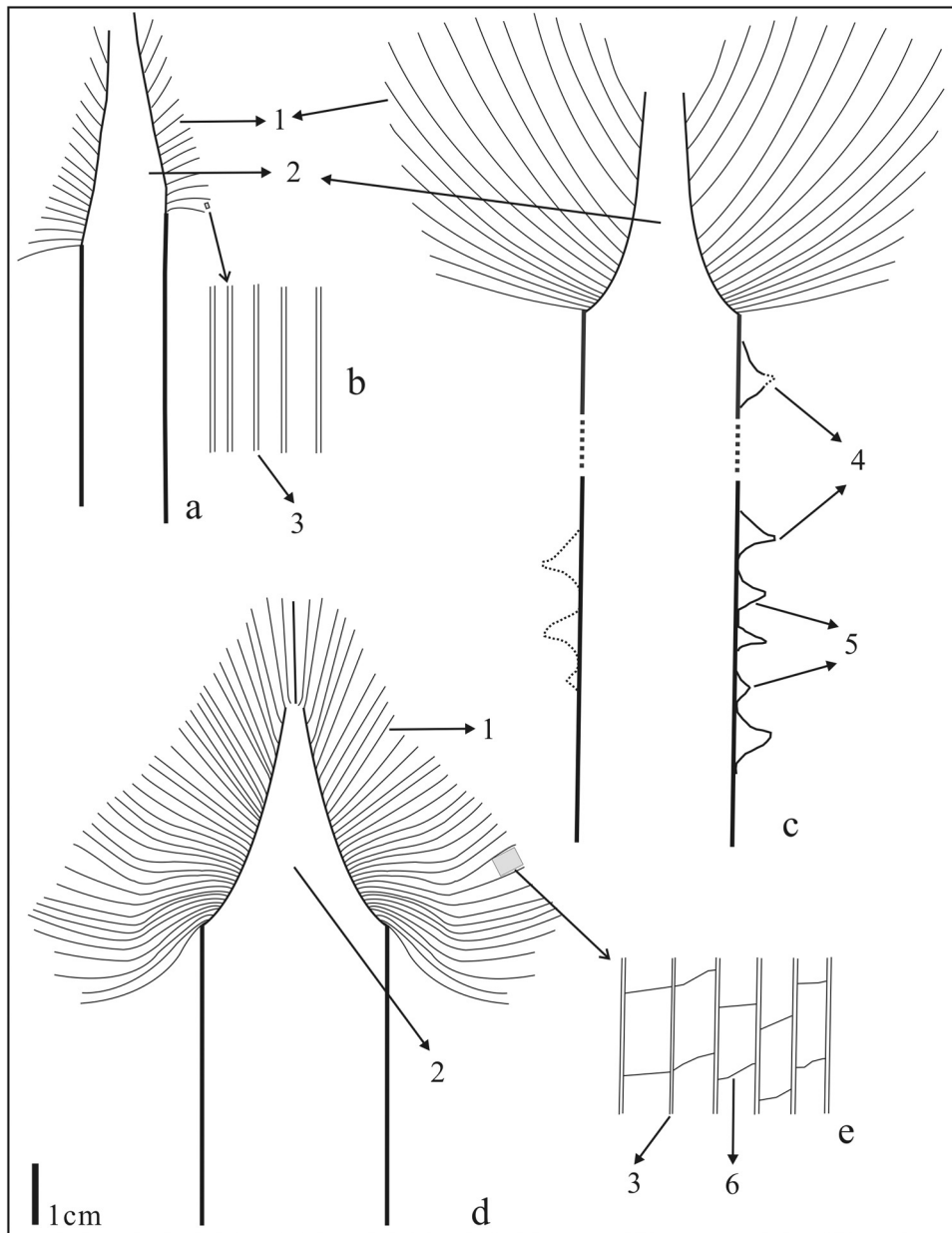


**Fig. 9.** Line drawings of the three fossil palms. a, b, *Chuniophoenix slenderifolia* sp. nov.; c, *Livistona roundifolia* sp. nov.; d, e, *Trachycarpus formosa* sp. nov. 1, the ribs of segments; 2, the costa; 3, the lateral veins; 4, the large spines; 5, the small spines; 6, the cross vein.

**Fig. 9.** Dessins au trait de trois palmiers fossiles. a, b, *Chuniophoenix slenderifolia* sp. nov.; c, *Livistona roundifolia* sp. nov.; d, e, *Trachycarpus formosa* sp. nov. 1, rubans de segments, 2, nervures, 3, veines latérales, 4, grandes épines, 5, petites épines, 6, veines croisées.

record. Although some palm fossils might have a similar leaf bases, such as *S. inquirenda* Knowlton and *S. grayanus* Lesquereux. *S. inquirenda*, from the Paleocene of America (Knowlton, 1917), differs in having more narrower segments (<5 mm). *S. grayanus*, which is known from Late Cretaceous to Eocene and described from many localities of North America (Lesquereux, 1878; Knowlton, 1930), can be distinguished by its broader segments (about 5 cm). *S. changchangensis* Guo, from the Eocene of Hainan, China (Guo, 1965; Zhou et al., 2013), is also characterized by the

cordate leaf base, but it differs in possessing a long straight costa (about 0.5 cm wide and 6 cm long) and a narrow petiole (1.5 cm in width).

The triangular costa is also represented in other extant palms, such as *L. chinensis*, *S. gretherae* H.J. Quero, *T. martianus* (Wall.) H. Wendland and some members of *Borassus*. The petioles of *L. chinensis* are characterized by the presence of robust spines (Fig. 5f). *S. gretherae* has more segments (50–60 pairs) and broader petioles (5–6 cm wide in the middle and 3–4 cm wide at the apex). The triangular

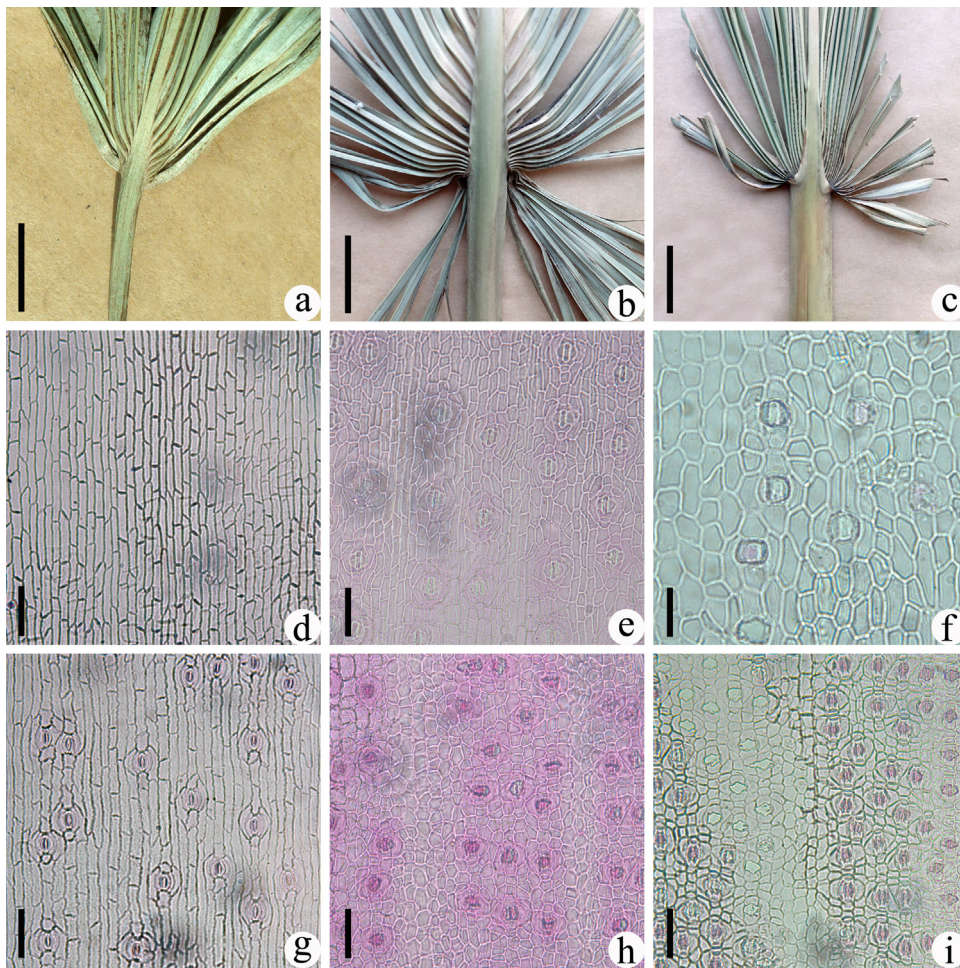


**Fig. 10.** (Color online.) Selected extant representatives. a: leaf of *Chuniophoenix humilis*, No. HNZWY-2013-XQZ; scale bar = 1 cm; b: leaf of *Sabal rosei*, No. HNZWY-2013-FLRZ; scale bar = 3 cm; c: leaf of *Sabal minor*, No. HNZWY-2013-XRZ; scale bar = 3 cm; d: adaxial cuticle of *Chuniophoenix humilis*; scale bar = 50  $\mu\text{m}$ ; e: abaxial cuticle of *Sabal rosei*; scale bar = 50  $\mu\text{m}$ ; f: abaxial cuticle of *Sabal minor*; scale bar = 25  $\mu\text{m}$ ; g: abaxial cuticle of *Chuniophoenix humilis*; scale bar = 50  $\mu\text{m}$ ; h: abaxial cuticle of *Sabal bermudana*; scale bar = 50  $\mu\text{m}$ ; i: abaxial cuticle of *Sabal mexicana*; scale bar = 50  $\mu\text{m}$ .

**Fig. 10.** (Couleur en ligne.) Représentants actuels sélectionnés. a : feuille de *Chuniophoenix humilis*, n° HNZWY-2013-XQZ ; échelle = 1 cm ; b : feuille de *Sabal rosei*, n° HNZWY-2013-FLRZ ; échelle = 3 cm ; c : feuille de *Sabal minor*, n° HNZWY-2013-XRZ ; échelle = 3 cm ; d : cuticule adaxiale de *Chuniophoenix humilis* ; échelle = 50  $\mu\text{m}$  ; e : cuticule abaxiale de *Sabal rosei* ; échelle = 50  $\mu\text{m}$  ; f : cuticule abaxiale de *Sabal minor* ; échelle = 25  $\mu\text{m}$  ; g : cuticule abaxiale de *Chuniophoenix humilis* ; échelle = 50  $\mu\text{m}$  ; h : cuticule abaxiale de *Sabal bermudana* ; échelle = 50  $\mu\text{m}$  ; i : cuticule abaxiale de *Sabal mexicana* ; échelle = 50  $\mu\text{m}$ .

costa of *T. martianus* is no more than 1 cm long (EBFC, 1991) and clearly differs from that of *T. formosa* sp. nov. Armed petioles are characteristic of *Borassus*, whose petioles all are heavily armed with teeth apart from *Borassus heineanus* Becc. (Dransfield et al., 2008; <http://www.palmweb.org/node/2>).

Anatomically, the new species and *T. martianus* all are characterized by hypostomatic leaves only with stomata on the abaxial cuticle (Fig. 8a and j), although *T. fortunei* is amphistomatic with rare stomata on the adaxial cuticle. Stomatal complexes of *T. formosa* sp. nov. are paratetracytic (Fig. 8a, d and g), similar in general morphology to those of the living species *T. fortunei* and *T. martianus* (Fig. 8h and j), although with some variations in the shapes of their subsidiary cells. Moreover, the stomatal distribution of the fossil and *T. fortunei* has a similar density on the abaxial cuticle (Fig. 8a and j). In particular, the petiole cuticles of the new species and *T. fortunei* all consist of

densely epidermal cells (Fig. 8c and f), which are rectangular or irregularly polygonal with rounded corners or oblique end walls. Thus, the fossil from Ningming is confirmed to have a close affinity to the living *Trachycarpus* based on the similarities of the morphological and cuticular characteristics. Although the petioles of the extant *Trachycarpus* are armed with minutely rounded or verrucate spines, the petiole spines are inconspicuous (Fig. 7f; Dransfield et al., 2008; EBFC, 1991). However, some extant palms share more or less similarities with the fossil in the cuticular characteristics (Appendix A), such as *Chuniophoenix* and *Sabal*. *C. hainanensis* Burret, which are also characterized by hypostomatic leaves, can be easily excluded from the fossil because of the attachment mode of basal segments (Fig. 3d). *S. rosei* (O.F. Cook) Becc., which is endemic to the coast of northwestern Mexico, has a long straight costa (Fig. 10b) and thus differs from the fossil. *S. minor* (Jacq.)

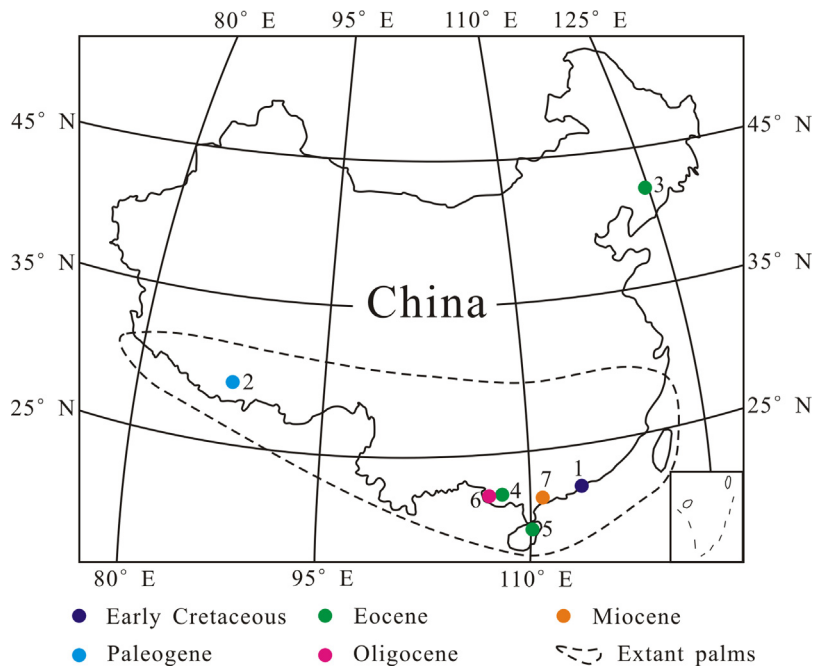


**Fig. 11.** (Color online.) Distribution of fossil and extant palms in China. 1. Pingzhou, Lidao, Hongkong (Zhou et al., 1990); 2. Lazi, Rikaze, Xizang (Tao, 1988; Appendix B); 3. Fushun, Liaoning (Endo, 1934); 4. Qitang, Shangsi, Fangchenggang, Guangxi (Guo, 1965); 5. Changchang, Ding'an, Haikou, Hainan (Guo, 1965; Zhou et al., 2013); 6. Chengzhong, Ningming, Chongzuo, Guangxi (This article); 7. Jigongling, Gaozhou, Maoming, Guangdong (Guo, 1965).

**Fig. 11.** (Couleur en ligne.) Distribution des palmiers actuels et fossiles en Chine. 1. Pingzhou, Lidao, Hongkong (Zhou et al., 1990); 2. Lazi, Rikaze, Xizang (Tao, 1988; Appendix B); 3. Fushun, Liaoning (Endo, 1934); 4. Qitang, Shangsi, Fangchenggang, Guangxi (Guo, 1965); 5. Changchang, Ding'an, Haikou, Hainan (Guo, 1965; Zhou et al., 2013); 6. Chengzhong, Ningming, Chongzuo, Guangxi (This article); 7. Jigongling, Gaozhou, Maoming, Guangdong (Guo, 1965).

Pers., which is native to the southeastern United States and characterized by a slightly asymmetrical leaf base, differs from the fossil in possessing a long narrow costa (Fig. 10c). Other *Sabal*, such as *S. bermudana* L.H. Bailey and *S. mexicana* Mart., can easily be distinguished from the fossil by their stomatal patterns (Fig. 10h and i).

Based on the morphological and cuticular comparisons with fossil and modern palms (Appendix A), we describe the present specimens as a new species, *T. formosa* sp. nov.

## 5. Biogeographical implications

Palms are characteristic components of tropical rain forests; thus, understanding the phylogeny and distribution of Chinese palms in time and space is fundamental in tracking the evolution of tropical rain forests in China. Although the palm flora in China has about 76 species in 17 genera, their fossils are relatively rare reported (Fig. 11; Appendix B). To date, there are 7 localities around China that have yielded palm fossils, with 15 species reported. The earliest fossils are represented by unarmed isolated segments. *Amesoneuron* sp., the earliest leaf, is described from the Early Cretaceous of Pingzhou, Hokong (the age of the Pingzhou flora is regarded as Albian based on plant macrofossils; Zhou et al., 1990), suggesting that palms have been established in China since the Early Cretaceous. Geographically, the occurrence of palm fossils from Xizang (Tao, 1988; Appendix B) indicates that the genus *Livistona* had reached the floras of western China by at least the Eocene. Palm remains are relatively abundant in the Eocene

Changchang Formation of Hainan (Zhou et al., 2013), with 7 morphospecies of fossil genera and 1 undefined species of the living genus *Livistona*. The high diversity may be an indication that palms were prevalent components of the Changchang flora. Other leaf fossils are also reported from the Eocene of Liaoning (Endo, 1934) and Guangxi (Guo, 1965). To date, this fossil record from Liaoning is at higher latitude than any other previous fossil records in China. So, the fossils from Liaoning, Guangxi, Xizang and Hainan show that palms in China had a wide distribution during the Eocene (Fig. 11; Appendix B). The narrow distribution of Chinese palms today (Fig. 11) may be linked to the deteriorating climates since the Eocene, such as more seasonal, arid and cooling climates (Baker and Couvreur, 2013b; Harley and Morley, 1995; Kissling et al., 2012; Pan et al., 2006). The present discovery in Guangxi represents the only palm fossils from the Oligocene of China and provides new fossil evidence about the palm biogeography in this country. The presence of *Chuniophoenix* fossil is significant because it is the first fossil record of the taxon. *Chuniophoenix* is endemic to southern China and northern Vietnam (Dransfield et al., 2008; EBFC, 1991). This report indicates that *Chuniophoenix* has occurred in China over a long geological period. In China, *Livistona* has been reported dating back to the Eocene, with two species recorded (Tao, 1988; Zhou et al., 2013; Appendix B). The occurrence of a *Livistona* fossil from Guangxi offers new data about the *Livistona* diversity in the Eocene of China, which indicates that Chinese *Livistona* has at least two species at that time. Extant *Trachycarpus* palms are native to Asia, from the

eastern Himalayas to eastern China. So far, no *Trachycarpus* fossil is reported from this country. The *Trachycarpus* fossil is the first record from its modern area of distribution and demonstrates that there was *Trachycarpus* growing in China since the Oligocene. In the Neogene, Chinese palm fossils were extremely rare, with only one leaf species from the Miocene of Guangdong (Guo, 1965). The lower frequency of palm fossils in the Neogene–Quaternary of this country may be a result of taphonomic biases or/and few paleobotanical studies. Better understanding of the palm biogeography in China requires further work that incorporates molecular analysis and new fossil records.

The origin and evolution of species-rich biomes raise fundamental questions regarding the diversification of palms (Bjorholm et al., 2006; Ling, 2002; Wei, 1995). The Areaceae is widespread yet shows high rates of endemism at varied spatial scales (Eiserhardt et al., 2011). The diversity of extant palms in Guangxi is one of the highest in China, both at the community and species levels (EBFC, 1991; Wei, 1997). Most of the palm vegetation types are found in Guangxi (EBFC, 1991; Wei, 1997), ranging from tropical to subtropical, temperate (e.g., *Chamaerops*), alpine (e.g., *Trachycarpus*) and xerophyte (e.g., *Phoenix*). Three subfamilies, namely, Coryphoideae, Calamoideae and Arecoideae, in 12 genera and 40 species, occur in Guangxi (EBFC, 1991; Wei, 1997). Only one species of *Trachycarpus* and two species of *Livistona* with costapalmate leaves are among the extant Guangxi flora (EBFC, 1991; Wei, 1997). However, all the palm fossils from Ningming are fan-shaped with no pinnate leaves recorded. It is in contrast to the extant palm flora of Guangxi, which is dominated by pinnate-leaved palms (EBFC, 1991; Wei, 1997). So, the occurrence of *C. slenderifolia* sp. nov., *L. roundifolia* sp. nov. and *T. formosa* sp. nov., may suggest that costapalmate palms in the palm flora of Ningming had relatively high diversity during the Oligocene.

The presence of coryphoid palms provides growing evidence that the Ningming flora had a greater diversity during the Oligocene. Preliminary floristic study indicates that the Ningming flora represents a subtropical evergreen forest with some tropical elements. Angiosperms are absolutely dominant in this flora, including Fabaceae, Lauraceae, Fagaceae, Moraceae, Areaceae, Hamamelidaceae, Betulaceae, Anacardiaceae, Simaroubaceae, Juglandaceae, Ulmaceae and Sapindaceae (Shi et al., 2012). So, the high species richness of costapalmate palms also supports the above-mentioned interpretation.

## 6. Conclusions

Palm fossils collected from the Oligocene deposits are assigned to three living genera and three new species, namely, *C. slenderifolia* sp. nov., *L. roundifolia* sp. nov. and *T. formosa* sp. nov. Our findings indicate that palms occurred in Guangxi over a longer geological period and suggest that a diversified palm flora was already present during the Oligocene in Guangxi. Additionally, the report provides a general survey of the occurrence of palm fossils in China, which provides important data on the biogeographical history of Chinese palms and is beneficial to

tracking the evolution of Chinese rainforests over geological time.

## Acknowledgments

We are grateful to Dr. Dian-Xiang Zhang and Dr. Fei-Yan Zeng (IBSC) for their permission to access the extant Areaceae material for comparison. We also thank the editor and three anonymous reviewers for their constructive comments and various help during reviewing and editing the manuscript. This research was financially supported by the National Basic Research Program of China (973 Program) (No. 2012CB822003); the National Natural Science Foundation of China (No. 41172022); the Funds of Key Laboratory of Economic Stratigraphy and Palaeogeography, Nanjing Institute of Geology and Palaeontology, CAS (No. Y421140303) and the Fundamental Research Funds for the Central Universities (No. lzujbky-2014-285).

## Appendix A. Supplementary data

Supplementary data associated with this article can be found, in the online version, at <http://dx.doi.org/10.1016/j.crpv.2015.03.005>.

## References

- Asmussen, C.B., Dransfield, J., Deickmann, V., Barfod, A.S., Pinaud, J.C., Baker, W.J., 2006. A new subfamily classification of the palm family (Areaceae): evidence from plastid DNA phylogeny. *Bot. J. Linn. Soc.* 151, 15–38.
- Baker, W.J., Couvreur, T.L.P., 2013a. Global biogeography and diversification of palms shed light on the evolution of tropical lineages. Diversification history and origin of regional assemblages. *J. Biogeogr.* 40, 274–285.
- Baker, W.J., Couvreur, T.L.P., 2013b. Global biogeography and diversification of palms shed light on the evolution of tropical lineages. Diversification history and origin of regional assemblages. *J. Biogeogr.* 40, 286–298.
- Bjorholm, S., Svenning, J.-C., Baker, W.J., Skov, F., Balslev, H., 2006. Historical legacies in the geographical diversity patterns of New World palm (Areaceae) subfamilies. *Bot. J. Linn. Soc.* 151, 113–125.
- Brown, S.H., 2013. *Bismarckia nobilis*, Family: Areaceae. University of Florida <http://lee.ifas.ufl.edu/Hort/GardenPubsAZ/Bismarck.palm.pdf>
- Chen, G.J., Chang, M.M., 2011. A new cyprinid from Oligocene of South China. *China Earth Sci.* 54, 481–492.
- Chen, G.J., Chen, Y.F., Kuang, G.D., Zhu, Q.P., 2004. Biostratigraphy of Tertiary fossil fishes from Ningming Basin, Guangxi. *Vertebr. Palasiat.* 42, 81–85 (in Chinese with English abstract).
- Chen, G.J., Fang, F., Chang, M.M., 2005. A new cyprinid closely related to *Cultrins* + *Xenocyprinus* from the mid-Tertiary of South China. *J. Vertebr. Paleontol.* 25, 492–501.
- Couvreur, T.L.P., Forest, F., Baker, W.J., 2011. Origin and global diversification patterns of tropical rain forests: Inferences from a complete genus-level phylogeny of palms. *BMC Biol.* 9, 44–55.
- Daghlian, C.P., 1978. Coryphoid palms from the Lower and Middle Eocene of southeastern North America. *Palaeontogr. Abt. B* 166, 44–82.
- Daghlian, C.P., 1981. A review of the fossil record of Monocotyledons. *Bot. Rev.* 47, 517–555.
- Daghlian, C.P., Dilcher, D.L., 1972. Middle Eocene sabaloid palms. *Proc. Indiana Acad. Sci.* 81, 94–95 (abstract).
- Dilcher, D.L., 1974. Approaches to the identification of angiosperm leafremains. *Bot. Rev.* 40, 1–157.
- Dransfield, J., Uhl, N.W., Asmussen, C.B., Baker, W.J., Harley, M.M., Lewis, C.E., 2005. A new phylogenetic classification of the palm family, Areaceae. *Kew Bull.* 60, 559–569.
- Dransfield, J., Uhl, N.W., Asmussen, C.B., Baker, W.J., Harley, M.M., Lewis, C.E., 2008. *Genera palmarum: the evolution and classification of palms*. Kew Publishing, Britain.



- Dutta, D., Ambwani, K., Estrada-Ruiz, E., 2011. Late Cretaceous palm stem *Palmoxylon lametaei* sp. nov. from Bhisli Village, Maharashtra, India. *Rev. Mex. Cienc. Geol.* 28, 1–9.
- EBCPC (Editorial Board for Cenozoic Plants of China), 1978. *Cenozoic Plants from China, Fossil Plants of China*, 3. Science Press, Beijing, pp. 159–161 (in Chinese).
- Editorial Board for Flora of China EBFC, 1991. *Flora of China*, 13. Science Press, Beijing, pp. 11–47 (in Chinese).
- Eiserhardt, W.L., Svenning, J.C., Kissling, W.D., Balslev, H., 2011. Geographical ecology of the palms (Arecaceae): determinants of diversity and distributions across spatial scales. *Ann. Bot.* 108, 1391–1416.
- Endo, S., 1934. The geological age of the Fushun Group, South Manchuria. *Proc. Imperial Acad. Sci.* 10, 486–489.
- Guo, S.X., 1965. On the discovery of fossil palms from the Tertiary Formation of Kwangtung and Kuangsi. *Acta Palaeontol. Sin.* 13, 598–605 (in Chinese).
- Harley, M.M., 2006. A summary of fossil records for Arecaceae. *Bot. J. Linn. Soc.* 151 (1), 39–67.
- Harley, M.M., Morley, R.J., 1995. Ultrastructural studies of some fossil and extant palm pollen, and the reconstruction of the biogeographical history of subtribes Iguanurinae and Calaminae. *Rev. Palaeobot. Palynol.* 85, 153–182.
- Henderson, A., 2009. *Palms of southern Asia*. Princeton Univ. Press, Princeton.
- Janssen, T., Bremer, K., 2004. The age of major monocot groups inferred from 800 + *rbcl* sequences. *Bot. J. Linn. Soc.* 146, 385–398.
- Kissling, W.D., Eiserhardt, W.L., Baker, W.J., Borchsenius, F., Couvreur, T.L.P., Balslev, H., Svenning, J.C., 2012. Cenozoic imprints on the phylogenetic structure of palm species assemblages worldwide. *PNAS* 109, 7348–7379.
- Knowlton, F.H., 1917. Geology and palaeontology of the Raton Mesa and other regions in Colorado and New Mexico. *U.S. Geol. Survey, Prof. Paper* 101, 288.
- Knowlton, F.H., 1930. The flora of the Denver and associated formations of Colorado. *U.S. Geol. Survey, Prof. Paper* 155, 36–39.
- Kuang, G.D., Chen, G.J., Chen, Y.F., Huang, Z.T., 2004. New information on the Tertiary biostratigraphy of the Ningming Basin, Guangxi. *J. Stratigr.* 28, 362–367 (in Chinese with English abstract).
- Kvaček, J., Herman, A.B., 2004. Monocotyledons from the Early Campanian (Cretaceous) of Grünbach, Lower Austria. *Rev. Palaeobot. Palynol.* 128, 323–353.
- Lesquereux, L., 1878. The Tertiary flora. *U.S. Geol. Survey, Terr.* 7, 107–122.
- Li, H.M., Chen, Y.F., Chen, G.J., Kuang, G.D., Huang, Z.T., 2003. Tertiary fossil winged fruits of *Palaeocarya* from Ningming of Guangxi, S. China. *Acta Palaeontol. Sin.* 42, 537–547 (in Chinese and English).
- Li, R., Qiu, D.Z., Li, G.R., 1995. Tertiary sedimentary facies and their controls on the reservoir quality in the Ningming Region, Guangxi. *Petrof. Paleogeogr.* 5, 40–45 (in Chinese with English abstract).
- Ling, Y.R., 2002. On the systematics, evolution, floristics and economic uses of palmae and its sister family, Calamaceae. *Bull. Bot. Res.* 22, 341–365 (in Chinese with English abstract).
- Ma, F.J., Xu, X.H., Li, R.Y., Wan, E., Sun, B.N., Yan, D.F., 2013. Dispersed cuticles from the Lower Cretaceous Wunite coal field in Inner Mongolia. *Acta Micropalaeontol. Sin.* 30, 244–262 (in Chinese with English abstract).
- Menon, M.V.K., 1964. *Palmocaulon raoi* possibly a new species of petrified palm petiole from Mohgaon Kalan Area in Madhya Pradesh. *Proc. Nat. Inst. India.* 30, 15–24.
- Newberry, J.S., 1898. The later extinct floras of North America. *U.S. Geol. Survey Monogr.* 35, 27–31.
- Ning, Z.S., Zhou, T.M., Hu, Y.K., Liang, Z.H., 1994. Tertiary in petroliferous regions of China. Petroleum Industry Press, Beijing (in Chinese).
- Pan, A.D., Jacobs, B.F., Dransfield, J., Baker, W.J., 2006. The fossil history of palms (Arecaceae) in Africa and new records from the Late Oligocene (28–27 My) of north-western Ethiopia. *Bot. J. Linn. Soc.* 151, 69–81.
- Read, R.W., Hickey, L.J., 1972. A revised classification of fossil palm and palm-like leaves. *Taxon* 21, 129–137.
- Shi, G.L., Zhou, Z.Y., Xie, Z.M., 2012. A new Oligocene *Calocedrus* from south China and its implications for transpacific floristic exchanges. *Am. J. Bot.* 99 (1), 108–120.
- Tao, J.R., 1988. Plant fossils from the Lêpuqu Formation in Lhazê County. Xi-zang and their palaeoclimatological significances. *Collected Papers of the Institute of Geology of the Chinese Academy of Science* 3, 223–238 (in Chinese).
- Tomlinson, P.B., 1979. Systematics and ecology of the Palmae. *Annu. Rev. Ecol. Syst.* 10, 85–107.
- Wang, Q.J., Xu, X.H., Jin, P.H., Li, R.Y., Li, X.Q., Sun, B.N., 2013. Quantitative reconstruction of Mesozoic paleoatmospheric CO<sub>2</sub> based on stomatal parameters of fossil *Baiera furcata* of Ginkgophytes. *Geol. Rev.* 59, 1035–1044 (in Chinese with English abstract).
- Wang, Q.J., Ma, F.J., Yang, Y., Dong, J.L., Wang, H.F., Li, R.Y., Xu, X.H., Sun, B.N., 2014. Bamboo leaf and pollen fossils from the Late Miocene of eastern Zhejiang, China and their phytogeological significance. *Acta Geol. Sin.* -Engl. 88, 1066–1083.
- Wang, Y.F., Tao, J.R., 1991. An introduction to a new system of terminology for plant cuticular analysis. *Chinese Bull. Bot.* 8, 6–13 (in Chinese with English abstract).
- Wang, W.M., Chen, G.J., Chen, Y.F., Kuang, G.D., 2003. Tertiary palynostratigraphy of the Ningming Basin, Guangxi. *J. Stratigr.* 27, 324–327 (in Chinese with English abstract).
- Wei, C.F., 1995. The geographic distribution of the Palmae. *J. Trop. Subtrop. Bot.* 3, 1–18 (in Chinese with English abstract).
- Wei, F.N., 1997. A taxonomic study on palm family from Guangxi. *Guihaia* 17, 193–205 (in Chinese with English abstract).
- Zhou, Z.Y., Li, H.M., Cao, Z.Y., Nau, P.S., 1990. Some Cretaceous plants from Pingzhou (Pingchau) Island, Hong Kong. *Acta. Palaeontol. Sin.* 29, 415–430 (in Chinese and English).
- Zhou, W.J., Liu, X.Y., Xu, Q.Q., Huang, K.Y., Jin, J.H., 2013. New coryphoid fossil palm leaves (Arecaceae: Coryphoideae) from the Eocene Changchang Basin of Hainan Island, South China. *Sci. China Earth Sci.* 56, 1493–1501.